Lithium borate crystals and glasses: How similar are they? A non-resonant inelastic X-ray scattering study around the B and O K -edges

Gerald Lelong, Laurent Cormier, Louis Hennet, Florent Michel, Jean-Pascal Rueff, James M Ablett, Giulio Monaco

Lithium borate crystals and glasses: how similar are they? A non-resonant inelastic X-ray scattering study around the B and O *K*-edges.

Gérald Lelong,[a,†] Laurent Cormier,[a] Louis Hennet,[b] Florent Michel,[a] Jean-Pascal Rueff,[d,e] James M. Ablett[d] and Giulio Monaco[c]

[a] *Institut de Minéralogie, de Physique des Matériaux et Cosmochimie (IMPMC),Sorbonne Universités – UPMC Univ Paris 06, UMR CNRS 7590, Muséum National d'Histoire Naturelle, IRD UMR 206, 4 Place Jussieu, F-75005 Paris, France*
[b] *Conditions Extrêmes et Matériaux: Haute Température et Irradiation, CNRS-UPR 3079, Orléans, France*
[c] *European Synchrotron Radiation Facility, 6 rue Jules Horowitz, BP 220, 38043 Grenoble Cedex, France*
[d] *Synchrotron SOLEIL, L'Orme des Merisiers, BP 48, Saint Aubin, 91192 Gif sur Yvette, France*
[e] *Laboratoire de Chimie Physique - Matière et Rayonnement, Université Pierre et Marie Curie / CNRS-UMR 7614, 75005 Paris, France*

[†] Corresponding author: gerald.lelong@impmc.upmc.fr

Abstract

The local environment of lithium borate glasses and their crystalline counterparts is investigated using non-resonant inelastic X-ray scattering (NRIXS) at energy losses corresponding to the B and O K-edges. Thanks to an extended series of lithium borate glasses and crystals, we have been able to finely interpret the local environments around boron and oxygen atoms in terms of coordination number, degree of polymerization of the borate network, superstructural units, and formation of non-bridging oxygens (NBOs). Even if a good local structural agreement between the glass and the crystal is found, an important structural discrepancy is found around the metaborate composition (50.mol% of Li_2O) rendering useless the use of the crystalline phase to describe the glassy state. In low alkali glasses, two subnetworks corresponding to a 'Li-rich' domain and a pure B_2O_3 domain containing boroxol rings have been evidenced. A spectral signature of the NBOs has also been evidenced in the π^* peak of the B K-edge, making NRIXS a useful method offering a series of spectral signatures which can be used as structural probes for up-coming high-temperature or high-pressure in-situ experiments.

1. Introduction

Alkali borate systems are experiencing a renewal of interest with the discovery of new crystalline phases containing transition metals,[1] [2] which are considered as potential new solid electrolyte materials for the next generation Li-ion batteries. Significant effort has then been devoted to understand the structural aspects of ionic conducting glasses in relation with their dynamical properties. However the understanding of the structural properties through the spectrum of light elements – such as lithium, boron and oxygen – remains a difficult question and sometimes an experimental challenge, especially for *in situ* measurements.

The structural diversity offered by alkali borates is impressive, as boron oxides can be built upon triangular BO_3 units, tetrahedral BO_4 units, or both. Another peculiarity of the alkali borate system resides in the formation of complex tridimensional structures known as superstructural units and composed of BO_3 and BO_4 building blocks. A large variety of superstructural units has been evidenced from a methodical analysis of the crystalline phases.[3–7] Even if the structure of glasses and other amorphous solids is characterized by the absence of long-range order, the alkali borate glass structure is also constituted by these superstructural units as demonstrated by the pioneering ^{11}B NMR studies in the mid-sixties,[8–12] and validated by vibrational spectroscopic methods.[13–16] This particularity makes alkali borates an intriguing example of glasses exhibiting significant crystalline-like medium-range order (MRO). Even after decades of research, the existence of this MRO through the formation of these superstructural units and the origin of their stabilization energy are still open questions, which requires additional experimental data accompanied by a solid theoretical support.[6] Nevertheless, the

specific arrangement of the different superstructures constrains geometrically the bond lengths and more importantly the B-Ø-B and O-B-O angular distributions, where Ø refers to a bridging-oxygen.[17] Since the bond lengths and the B-Ø-B angles are mainly dictated by the $^{[3]}B/^{[4]}B$ ratio, the local structure around the boron atoms will be *a priori* less sensitive to the structure of the superstructural units. On the contrary, the local environment around the oxygen atom is potentially more suited to probe the medium-range order since it is sensitive to the B-Ø-B angle. Studying the structure of glasses through the spectrum of the ligands allows one to obtain a complementary vision of the glassy structure through the understanding of the connectivity of the boron polyhedra and their spatial organization. A variety of spectroscopic techniques has been used to selectively probe the oxygen environment: X-ray photoelectron spectroscopy (XPS), electron energy loss spectroscopy (EELS),[18–20] X-ray absorption spectroscopy (XAS) and ^{17}O nuclear magnetic resonance (NMR), which are all well suited for such an investigation. However, XPS, EELS and O *K*-edge XAS require ultra-high vacuum conditions, which often appears as an important limitation for *in situ* measurements. The use of isotopically enriched samples in NMR can also be a limitation for studying natural samples or for systematic studies.

Studying glasses through light elements, such as boron or oxygen, can be an experimental challenge. Thankfully, the rapid development of non-resonant inelastic X-ray scattering (NRIXS) – also known as X-ray Raman Spectroscopy - allows the investigation of electronic transitions of low Z elements. Using high-energy incident X-rays, NRIXS is bulk sensitive and can be used as a substitute for ultrasoft X-ray absorption spectroscopy for the *K*-edges of light elements ($Z < 18$), which has a low penetration depth. It is then perfectly suited for studying changes in the electronic structure and consequently in the local atomic structure, as demonstrated by recent studies on a wide variety disordered systems such as water, borates, silicates, germanates…[21–26] Interestingly, the *K*-edges are obtained in the energy loss domain, allowing to probe several edges simultaneously similarly to EELS.

By coupling the precise knowledge of the different lithium borate crystalline structures with the experimental B and O *K*-edges NRIXS spectra on an extended series of lithium borate glasses and crystals, we have been able to finely interpret the local environments around boron and oxygen atoms in terms of coordination number, polymerization degree of the borate network, superstructural units, formation of non-bridging oxygens (NBOs), and develop a series of spectral signatures which can be used as structural probes for up-coming high-temperature or high-pressure experiments.

2. Experimental details

a. Synthesis

Lithium borate glasses were synthesized by melting weighted mixtures of high purity alkali carbonate and boric acid in a Pt/Rh crucible at 1000°C during 20 minutes. Six different glasses were prepared with the following molar compositions: $(1-x)Li_2O$-xB_2O_3, where x = 0.3, 0.5, 0.66, 0.75, 0.9 and 1, denoted L7B3 ($7Li_2O$-$3B_2O_3$), LB (Li_2O-B_2O_3), LB2 (Li_2O-$2B_2O_3$), LB3 (Li_2O-$3B_2O_3$), LB9 (Li_2O-$9B_2O_3$) and v-B_2O_3, respectively.

As reference samples, six lithium borate crystals were prepared with the following molar compositions: $3Li_2O$:$11B_2O_3$ ($Li_3B_{11}O_{18}$), Li_2O:$2B_2O_3$ ($Li_2B_4O_7$), Li_2O:B_2O_3 ($LiBO_2$), $3Li_2O$:$2B_2O_3$ ($Li_6B_4O_9$), $2Li_2O$: B_2O_3 (α-$Li_4B_2O_5$) and $3Li_2O$:B_2O_3 (Li_3BO_3). The synthesis procedure of these lithium borate crystals has been described previously.[27] The purity of the crystalline phases for each compound was checked using powder X-ray diffraction (Cu Kα radiation on a Panalytical X'pert pro MPD). Diffractograms were compared to the literature.[28–32]

b. NRIXS Spectrometers

i. ID16 Beamline – ESRF

The NRIXS experiments on lithium borate glasses were carried out at the ID16 Inelastic X-ray beamline at European Synchrotron Radiation Facility (ESRF).[33] The incident beam was monochromatized with Si(111) and Si(220) monochromators and the beam focused to 115 (H) × 40 (V) μm^2. The scattered radiation was analyzed with nine bent Si(660) analyzers (R = 1 m) and detected with a photon-counting MAXIPIX bidimensional pixel detector.[34] Spectra were collected by scanning the incident energy while maintaining the analyzers energy at 9.6885 keV, so that the energy transfer was scanned around the B K-edge at 190 eV and the O K-edge at 535 eV. The total energy resolution of the setup was 0.7–0.8 eV (FWHM) as measured by fitting a Gaussian profile to the quasi-elastic scattering peak. All the measurements were made at an average scattering angle of 30° in 2θ. Under these conditions all 9 analyzers are in a low exchanged momentum q configuration (q ~ 2.54 $Å^{-1}$) and their signal can be summed. An accumulation time of at least 2h was necessary to achieve good statistics. A background subtraction has been achieved and each spectrum has been normalized to surface area.

ii. GALAXIES Beamline – SOLEIL

The measurements of the crystalline samples were performed on the GALAXIES beamline at the SOLEIL Synchrotron.[35] The incident energy was monochromatized with a Si(111) double – crystal monochromator and the beam focused to ~100 (H) x 30 (V) μm^2. The scattered radiation was analyzed with 4 spherical Si(660) analyzers (R = 1m) and detected with an avalanche photodiode. Spectra were collected by keeping the analyzers fixed at their backscattering energy of 9.720 keV (Bragg angle ~ 86°) while scanning the incident X-ray energy. For example, the O K-edge at 535 eV was measured by varying the incident X-ray energy around 10.255 keV. The total energy resolution of the setup was ~1.5 eV (FWHM), as measured by fitting a Gaussian profile to the quasi-elastic scattering peak. All

the measurements were made at an average scattering angle of 40° in 2θ. Under these conditions all 4 analyzers are in a low exchanged momentum q configuration (q ~ 3.37 Å^{-1}) and their signal can be summed. An accumulation time of at least 5h was necessary to achieve good statistics. A background subtraction has been achieved and each spectrum has been normalized to surface area.

3. Results and discussion

A. SHORT RANGE ORDER

In order to obtain a full appreciation of the modification of the local structure upon the addition of lithium oxide, six lithium borate glasses spanning over a large alkali concentration (0 to 70 mol.%) were considered. All samples were measured at room temperature except L7B3 (measured at T = 450°C) and the O *K*-edge of LB3 (measured at T = 250°C). The B and O *K*-edges spectra for the six glasses are shown on the Figure 1. Unambiguously, the addition of Li_2O into B_2O_3 leads to drastic changes in the shape of the signal at both energies.

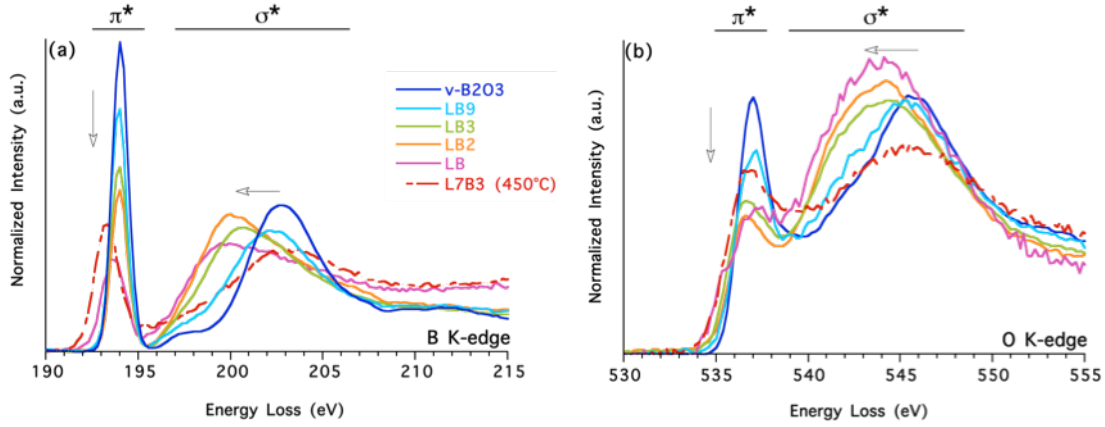

Fig. 1: *(a) Effect of Li_2O content on both (a) B K-edge and (b) O K-edge NRIXS spectra of six lithium borate glasses: v-B_2O_3 (blue), LB9 (cyan), LB3 (green), LB2 (orange), LB (pink) and L7B3 (red). All the spectra were obtained at room temperature except those for L7B3 (measured at 450°C for both B and O K-edges) and for LB3 (measured at 250°C for O K-edge only).*

Impact of Li_2O on the B K-edge spectrum

As previously described,[36]·[37] the B *K*-edge of glassy B_2O_3 (Fig. 1a) shows two main features associated to three-fold coordinated boron atoms ($^{[3]}$B): (i) a narrow and intense peak at 194 eV related to transitions of a core boron 1*s* electron to an unoccupied boron antibonding π^* orbital of the BO_3 structural units, and (ii) a broader peak centered around 203 eV corresponding to the transition of a B 1*s* electron to an unoccupied B-O σ^* antibonding orbital. Upon the addition of lithium oxide, the intensity of the π^* peak at 194 eV decreases and the σ^* peak shifts towards the lower energies with the appearance of a new absorption peak centered around 198-200 eV. The presence of this peak is a

clear indicator of the increasing number of fourfold coordinated boron atoms as observed in BPO_4 or in pressurized borate glasses.[36]·[38]·[23] The modifications of the B *K*-edge are then indicative of a gradual boron coordination change from neutral $BØ_3$ units to negatively charged tetrahedral $BØ_4$ units.[36,39]·[13] Beyond the diborate composition, *i.e.* for a Li_2O content above 50 mol.%, the intensity of the peak at 200 eV decreases in favor of the σ^* peak at 203 eV in correspondance with the formation of planar BO_3 units containing NBOs.[6]·[13] This is accompanied by a slight shift of about 0.4-0.5 eV of the π^* peak position towards lower energy, which is observed for glasses as well as crystalline phases (Fig. 1a and 2a). As previously described, these six crystalline phases allow following the disruption of the borate network with increasing lithium content.[27] As the crystalline structures are known, it is possible to link the local structure of boron with the observed spectral features. By plotting the average $^{[3]}$B-O bond distance as a function of the π^* peak position for these six lithium borate crystals (Fig. 2b), it is possible to define two domains: a first one around 194.5 eV related to a fully polymerized borate network, and a second one - around 194.1eV and spreading on a wider energy range - related to depolymerized borate networks. In this latter case, a gradual shift toward lower energy is observed when the content of NBOs increases. Since the π^* feature is solely related to $^{[3]}$B, it is interesting to look at the evolution of the $^{[3]}$B-O bond length with the NBO content only. Even if the average $^{[3]}$B-O value is relatively constant over the whole range of concentration (1.37-1.38 Å), the average $^{[3]}$B-NBO bond distance increases with the increase of NBO content (Fig. 2c). With a longer B-NBO distance, the antibonding π^* orbital of the BO_3 units is lowered leading to a shift of the π^* peak towards lower energies. This core level shift, which is low but accessible with a relatively standard resolution, is then a spectral feature of the presence of one (or several) NBO(s) around a three-fold-coordinated boron. The B *K*-edge by means of its π^* feature appears to be a sensitive probe of the short-range order, which opens the way to a potential new series of studies on depolymerized borates such as those envisaged for future batteries.[1,2]

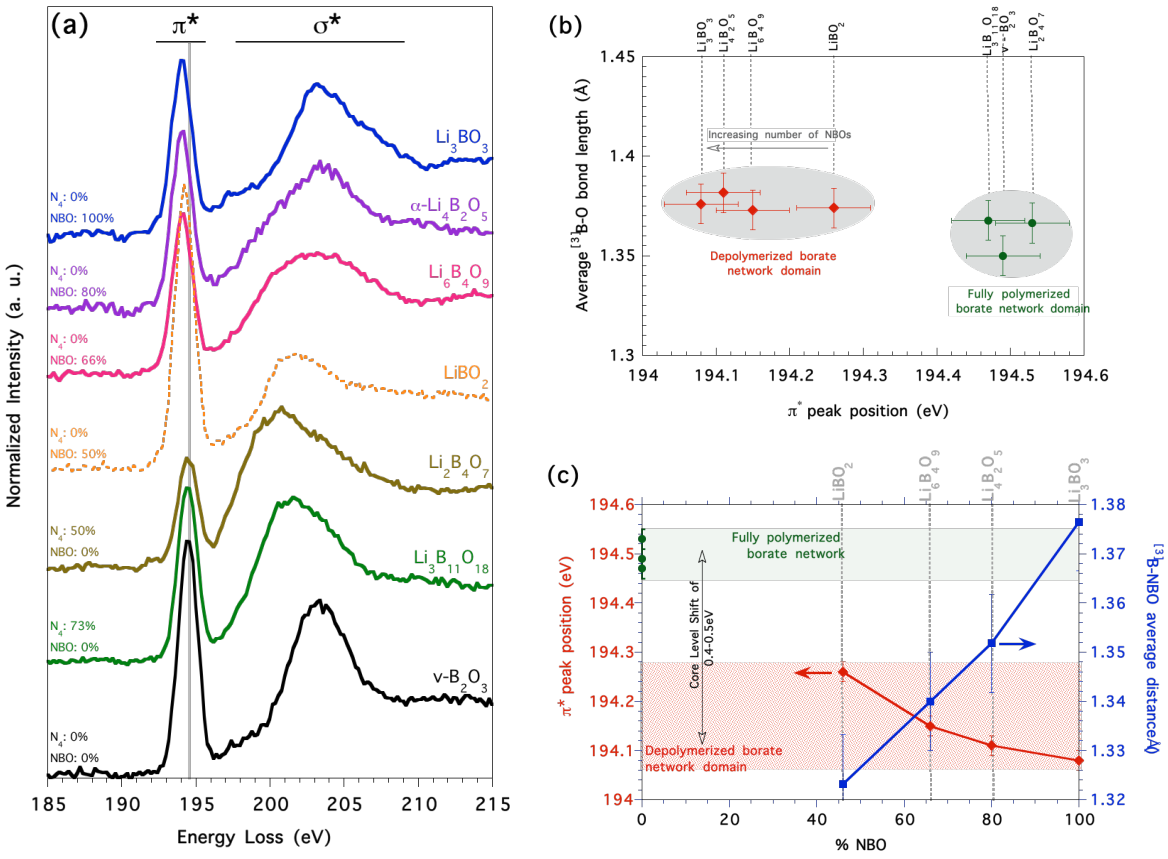

Fig. 2: *(a) B K-edge NRIXS spectra for the six crystalline compounds of the Li_2O-B_2O_3 system. Li content increases from bottom to top, starting from a Li_2O concentration of 21 mol.% in $Li_3B_{11}O_{18}$ (green) to 75 mol.% in Li_3BO_3 (blue). B K-edge of vitreous B_2O_3 (black) is shown as an example of a pure 3-fold-coordinated boron in a fully coordinated network. The gray line indicates the position of the π* peak for v-B_2O_3. Proportion of NBO and four-fold coordinated boron (N_4) are also given for each composition. (b) Evolution of the average $^{[3]}$B-O bond length as a function of the π* peak position for the same compounds. (c) Evolution of both the average $^{[3]}$B-NBO distance (blue) and of the π* peak position as a function of NBO content. The π* peak position is given for fully polymerized structures (v-B_2O_3, $Li_3B_{11}O_{18}$ and $Li_2B_4O_7$ - green) and for depolymerized structures ($LiBO_2$, $Li_6B_4O_9$, $Li_4B_2O_5$ and Li_3BO_3 – red).*

Following a method described elsewhere,[36] the $^{[3]}$B fraction (N_3) in the glass can be determined by dividing the surface area of the π^* peak of the lithium borate glass by the surface area of the π^* peak of a reference sample containing 100% of $^{[3]}$B, *i.e.* v-B_2O_3. Prior to any calculation, all spectra were normalized to surface-area in the energy range 185 – 218 eV. Figure 3 shows the evolution of the proportion of $^{[4]}$B ($N_4 = 1 - N_3$) as a function of Li_2O content compared with ^{11}B NMR and neutron diffraction (ND) data found in the literature.[10–12,40–45] The proportion of $^{[4]}$B in glassy lithium borate follows a non-linear behavior as a function of Li_2O content with a maximum around 30-40 mol.% Li_2O. The good agreement between the present values extracted from NRIXS spectra and those extracted from NMR data demonstrates the reliability of XRS to deduce the coordination number of boron atoms.

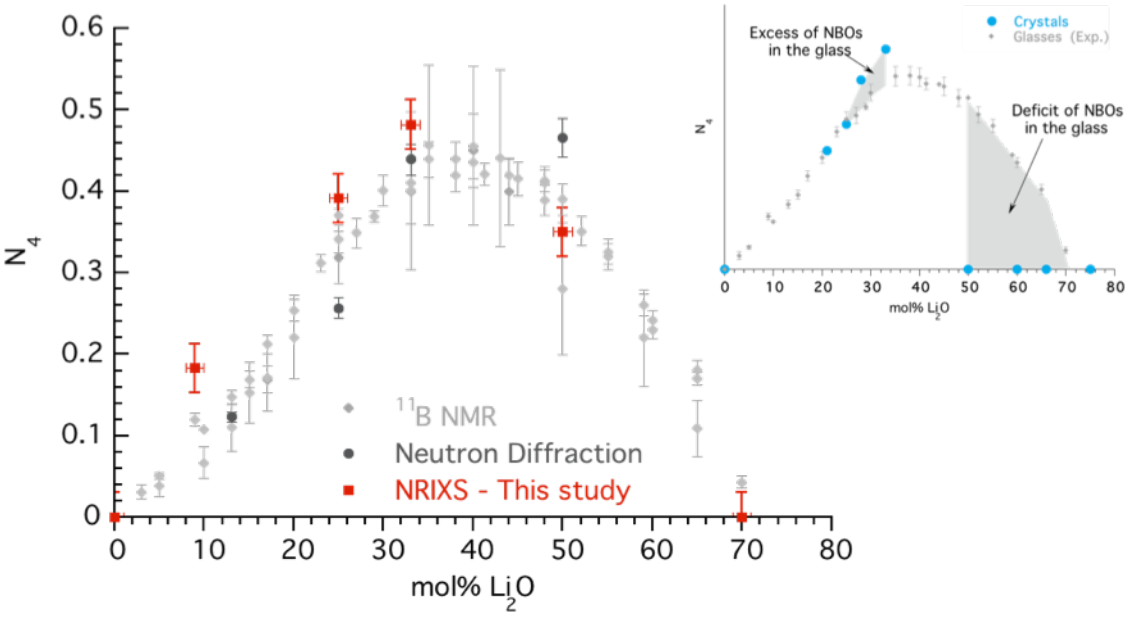

Fig. 3: *Compositional dependence of the proportion of fourfold coordinated boron (N_4) in lithium borate glasses at room temperature from present work (red filled squares) and from ^{11}B NMR (light gray filled diamonds) and from neutron diffraction (dark gray filled circles) data.*[10–12,40–45] *The inset shows a comparison of N_4 values as a function of lithium content for glasses (gray filled diamonds) and crystals (blue filled circles). The shaded areas highlight concentration domains where discrepancies are found between glasses and crystals.*

Values of N_4 have been deduced from the crystal structures of the different phases under study and are plotted as a function of Li_2O content accompanied with the values deduced by NMR and NRIXS (Fig. 3 - inset). While at low Li_2O content there is almost no differences in the *N4* fraction between the glasses and the crystals, a clear divergence occurs around 25mol.% Li_2O. In this part of the diagram, the number of $^{[4]}$B is higher in the crystalline phases than in the glasses, meaning an excess of NBOs for the glasses in this concentration range compared to the crystalline counterparts. This difference of behavior may originate from the disordered nature of glass, which has to topologically accommodate its structure to internal constraints arising from the geometry of polyhedra (B and Li) and also from the nature of the involved superstructural units. Unfortunately, no information can be deduced between 33 and 50 mol.% of Li_2O since no crystalline phase is known in this range. Above 50 mol.% Li_2O, the crystalline phases do not contain any four-fold-coordinated boron, and consequently N_4 is null for all the high Li_2O concentrations. Intriguingly, the glass still keeps a large number of $^{[4]}$B on a relatively wide concentration domain ranging from 50 to 70 mol.% Li_2O. This indicates a deficit of NBOs in glasses in comparison with their crystalline counterparts. This important structural difference is more difficult to explain with simple arguments related to wider distributions of bond lengths or angles.

Impact of Li_2O content on the O K-edge spectrum

Figure 1(b) shows the evolution of the O *K*-edge NRIXS spectrum of the same alkali borate glasses as a function of Li_2O content. The O *K*-edge spectrum of v-B_2O_3 is characterized by two main features: a narrow peak π^* at 537 eV and a broad peak σ^* centered around 546 eV corresponding to electronic transitions from a 1s core state to unoccupied antibonding π^* and σ^* orbitals of the BO_3 units. Both peaks are related to two-fold-coordinated oxygen atoms with a relatively narrow $^{[3]}$B–Ø–$^{[3]}$B angle dispersion.[38]

Upon the addition of lithium, the π^* feature decreases in intensity and σ^* shifts to lower energies. Despite the lack of theoretical work on the interpretation of the O *K*-edge spectrum of v-B_2O_3, it is clear that the first peak at 537 eV is very sensitive to the $^{[3]}$B-Ø-$^{[3]}$B angle. The narrowness of this peak is indicative of the homogeneity of the local structure around the oxygen atoms in terms of the Ø-$^{[3]}$B bond length and the $^{[3]}$B-Ø-$^{[3]}$B angular distribution. In view of the evolution of N_4 as a function of Li_2O content (Fig. 3), the broad band σ^* seems to be sensitive to both BO_3 and BO_4 units and consequently to the $^{[3]}$B-Ø-$^{[3]}$B, $^{[3]}$B-Ø-$^{[4]}$B and $^{[4]}$B-Ø-$^{[4]}$B angles. Nevertheless, the increasing intensity between 540 and 545 eV when Li_2O is added indicates a sensitivity of this part of the spectrum to the fourfold coordinated boron. We can also note the presence of a shoulder at 535 eV for the LB and L7B3 glasses, which is related to the presence of NBOs, whose spectral signature has been demonstrated by Density Functional Theory (DFT) calculations and NRIXS.[27] The appearance of these NBOs in the glass is a clear evidence of the progressive disruption of the borate network. Even if a quantification of NBOs is difficult to achieve, the measured intensity at 535 eV is however indicative of the concentration of NBOs present in the sample. We will see later that by comparing O *K*-edge spectra for glasses and crystals,[27] a significant amount of NBOs can be inferred at high Li_2O concentrations.

B. MEDIUM RANGE ORDER – CRYSTALS VS. GLASSES

By studying both the B and O *K*-edges independently, structural information has been deduced about the borate backbone in terms of boron coordination number and NBOs. The alkali borate structure is rendered complicated by the combination of the two boron coordination states ($^{[3]}$B and $^{[4]}$B) and also by the formation of superstructural units. The latter arrangements, if discernable in the glass structure, would bring important information on MRO. To do so, a selection of six crystalline lithium borates are used as reference for well-defined superstructural units: pentaborate unit ($B_5O_6Ø_4^-$), triborate units ($B_3O_3Ø_4^-$), diborate unit ($B_4O_5Ø_4^{2-}$), pyroborate unit ($B_2O_5^{4-}$), orthoborate (BO_3^{3-}) unit, and the metaborate chains $(BOØ_2^-)_\infty$ found in $LiBO_2$.[27] The B and O *K*-edges NRIXS spectra of four glasses (LB9, LB2, LB and L7B3) are plotted together with compositionally equivalent crystals. (Fig. 4)

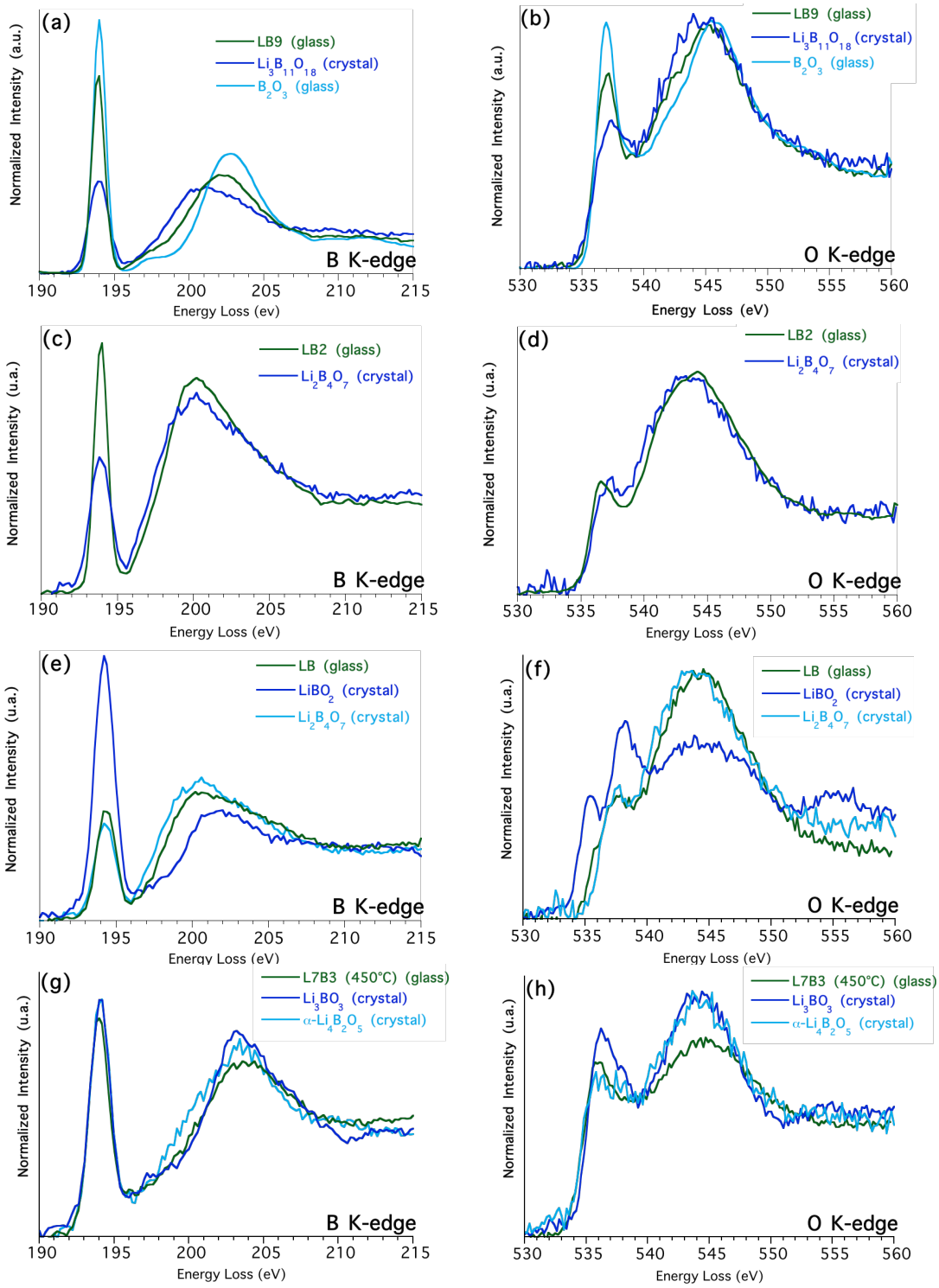

Fig. 4: *B K-edge (left) and O K-edge (right) spectra of the four lithium borate glasses (LB9, LB2, LB and L7B3) (green curves) and their respective crystalline phases (blue curves).*

LB9 (enneaborate composition)

The B and O *K*-edges spectra of LB9 are plotted with those for the crystals with the closest composition, i.e. v-B_2O_3 (0 mol.%) and $Li_3B_{11}O_{18}$ (21 mol.% Li_2O) (Fig. 4a and 4b). Clearly, neither the spectra for v-B_2O_3 nor the spectra for $Li_3B_{11}O_{18}$ match with the LB9 ones for both edges. Nevertheless, the NRIXS spectra of the glass show an intermediate behavior between those of the two compounds. Interestingly, if we calculate a linear combination of the spectra of v-B_2O_3 and $Li_3B_{11}O_{18}$ for both edges (Fig. 5), we find an almost perfect agreement with the LB9 glass, meaning that both the boron and oxygen environments are consistent with the local environments found in glassy B_2O_3 and $Li_3B_{11}O_{18}$. Consequently, LB9 has to be constituted by the superstructural units present in these two compounds, *i.e.* boroxol rings, triborate and pentaborate units. The presence of boroxol rings at this composition would be coherent with the peculiar optical properties observed in low-alkali glasses containing Co, Ni, or Zn.[46],[47],[48] In these glasses, the transition element shows unusual coordination numbers - such as $^{[6]}$Co, $^{[6]}$Ni and $^{[6]}$Zn, which requires the presence of a rigid structure for allowing an alignment of several edge-sharing octahedral sites. This interpretation is also supported by the intense Raman peak at 807 cm^{-1} observed at these low-alkali compositions, which is related to the breathing mode of oxygens in boroxol rings.[49] The good agreement between the linear combination and LB9 spectra on both edges also suggests that two sub-domains could coexist in the glass: an "alkali-rich" domain and a pure B_2O_3 domain containing the boroxol rings. The two sub-domains would be then representative of the two stable compounds located on both side of LB9, *i.e.* v-B_2O_3 and $Li_3B_{11}O_{18}$, whose the compositions appear to roughly correspond to the boundaries of the sub-liquidus immiscibility domain ranging from 0 to 18 mol.% in the case of lithium.[50] The atomic structure of $Li_3B_{11}O_{18}$ is in favor of such interpretation, since it already contains a *Li-rich* domain and an *alkali-free* domain whose the size of this latter can reach 10 Å × 5 Å in each unit cell. (Fig. 6) These two sub-domains could favor a demixing of the glass.

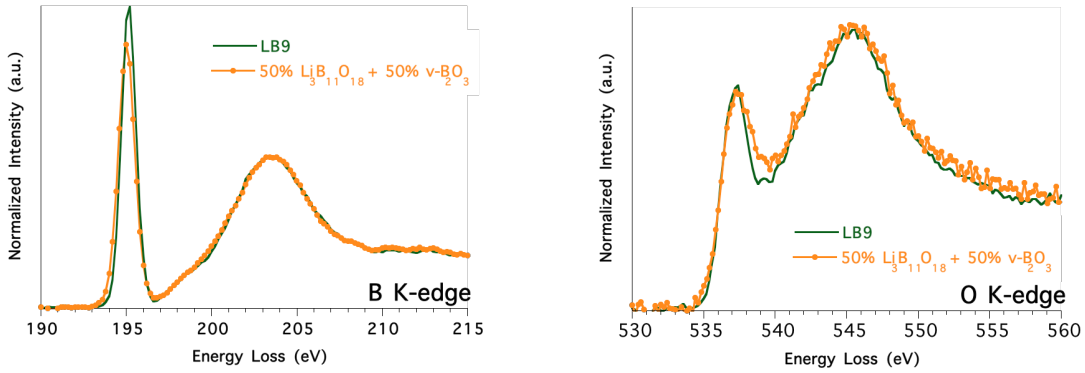

Fig. 5: *B K-edge (left) and O K-edge (right) NRIXS spectra of the LB9 glass (green) accompanied with the linear combination of of v-B_2O_3 and $Li_3B_{11}O_{18}$ spectra (orange).*

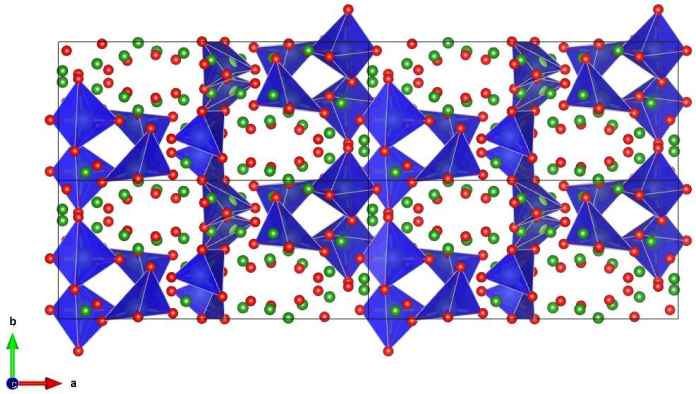

Fig. 6: *Structure of $Li_3B_{11}O_{18}$, viewed along [001]. O and B atoms are colored red and green respectively, while Li polyhedra are colored in blue.*

LB2 (diborate composition)

As mentioned above, the diborate composition contains the largest fraction of BO_4^- units in lithium borate glasses and crystals, with Li ions occurring in a charge compensating position. The O and B *K*-edges spectra of both the glass (LB2) and the corresponding crystal ($Li_2B_4O_7$) are shown on the Figures 4c and 4d, respectively. Except the resolution difference between the glass and the crystal due to the different resolutions of the ID16 and GALAXIES spectrometers, the overall agreement is rather good for both edges. The NRIXS spectra of LB2 and $Li_2B_4O_7$ are then indicative of analogous borate networks in terms of B–Ø bond lengths, Ø–B–Ø angular distributions and connectivity between the boron polyhedra - with comparable B–Ø–B angular distributions. Since the crystal structure of $Li_2B_4O_7$ is solely constituted of diborate units, LB2 is then largely composed by these groups, implying a highly polymerized glass. The slight differences are ascribable to distortions of the B and O sites related to the glassy network and also to the presence of few NBOs, as suggested by different studies,[49] even though the signature of NBOs is hardly discernible on the O *K*-edge spectrum. The higher disorder is supported by the higher mass density of $Li_2B_4O_7$ in comparison with LB2. (Fig. 7) The closeness of both glassy and crystalline structures is coherent with both the infrared and Raman study of Kamitsos *et al.*[13][49] and the NMR study of Chen *et al.*[51]. This latter work suggests that the structural similarities favor the homogeneous nucleation of the crystalline phase in LB glass.

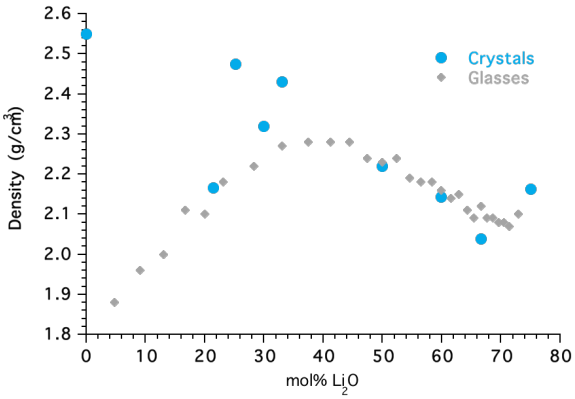

Fig. 7: *Density of lithium borate glasses (gray filled circles) and crystals (blue filled circles) as a function of Li_2O content.*[7]

LB (metaborate composition)

The NRIXS B and O *K*-edges spectra of LB and $LiBO_2$ are shown in Figures 4e and 4f. Both edges show clear discrepancies highlighting the lithium metaborate anomaly, which corresponds to dissimilar local structures between the glass and the corresponding crystalline phase.[6],[52] Surprisingly, their densities are almost identical even with radically different structures, meaning that they have both optimized their atomic packing. (Fig. 7) As a reminder, $LiBO_2$ is constituted by infinite chains of $B\emptyset_2O^-$ units, *i.e.* a BO_3 unit containing one NBO. The signature of NBOs is clearly visible at 535 eV on the O *K*-edge spectrum. Considering the B *K*-edge spectrum for LB, it is clear that the proportion of $^{[4]}B$ is still important, with an estimated value of ~35%. Since NBO associated with BO_4 units are energetically unfavored, the presence of four-fold coordinated boron in the glass structure indicates the presence of six-membered rings (O-B-O-B-O-B). Indeed, a good agreement is observed for the NRIXS spectra of LB and $Li_2B_4O_7$, which is consistent with a large proportion of diborate units which are still reminiscent in the glass. Alternatively, no superstructural units involving BO_4 units exist in the $LiBO_2$ crystal and important differences are seen between the NRIXS spectra of LB and $LiBO_2$. These results indicate that six-membered rings are energetically stabilized at this glass composition. More intriguingly, it would seem that these small rings are kept in the glass structure over a wide Li_2O concentration range (0 - 70mol.%), if one is based on the fact that BO_4 tetrahedra are always involved in at least one six-membered rings in the crystalline structures. This interpretation stands only if both glasses and crystals share a common pool of superstructural units. It is known from calculations, that small rings have a stabilizing effect on borate structures, such as boroxol rings in pure glassy B_2O_3.[53,54] These six-membered rings, which are present in almost every commonly occurring superstructural units reported,[6] have a key structural role by tiling the tridimensional borate network in such a way to limit internal constraints.[3,4] As discussed by Wright, the network modifying cations do not passively occupy sites formed by the surrounding vitreous network, but they modify their environment to suit their own particular requirements.[4] By keeping this in mind, it is then pertinent to look at the lithium environment in $Li_2B_4O_7$ and $LiBO_2$. Interestingly, $Li_2B_4O_7$ is constituted by corner-sharing lithium trigonal bipyramids, whereas $LiBO_2$ is constituted by edge-sharing trigonal bipyramids. This means that the formation of edge-sharing polyhedra is energetically more expensive than the formation of corner-sharing polyhedra owing to electrostatic interactions. It is then more energetically effective for the LB glass structure to be close to the $Li_2B_4O_7$ structure, even with the creation of few NBOs, rather than achieving a more opened $LiBO_2$-like structure with a large proportion of NBOs.

L7B3

Finally, the B and O *K*-edges NRIXS spectra of L7B3 accompanied with those of Li_3BO_3 and α-$Li_4B_2O_5$ are shown on the Figure 4g and 4h, respectively. We have to mention here that this glass is

difficult to synthesize because of the very high amount of Li_2O. This sample has then been measured at 450°C in an aerodynamic levitation device coupled with laser heating.

The spectral similarities between L7B3 and the two crystalline phases indicate that L7B3 is constituted by a mixture of pyroborate and orthoborate units. Considering the B *K*-edge spectra, the similarities are slightly higher for Li_3BO_3 than for α-$Li_4B_2O_5$, suggesting that the glass structure is mostly constituted by orthoborate units (BO_3^{3-}). The O *K*-edge spectra present a well defined feature at 535 eV, ascribed to NBOs. The high peak intensity indicates the quasi exclusive presence of NBOs attached to BO_3 units, which is characteristic of pyroborate and orthoborate units. This glass is then an example of an invert glass. The L7B3 composition has been measured at 450°C, in the supercooled region. At this temperature, the liquid structure is already similar to the structure of Li_3BO_3 and α-$Li_4B_2O_5$. This similarity could explain the difficulty to quench a glass of this composition since few structural rearrangements are required to achieve a crystalline organization.

Finally, the complete set of superstructural units found in lithium borate glasses and crystals is summarized in Figure 7.

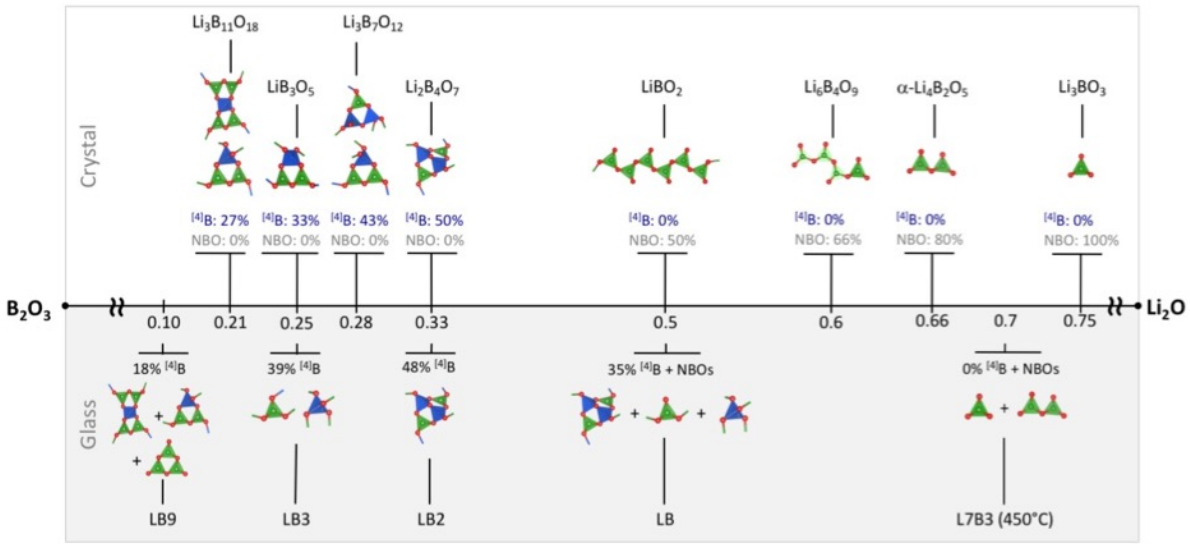

Figure 7: *Summary of the superstructural units found in glasses (bottom) and crystalline phases (top) at ambient conditions for the Li_2O-B_2O_3 system.*

4. Conclusion

This study highlights the interest to probe simultaneously both B and O *K*-edges in order to benefit from their different sensitivities. The NRIXS B *K*-edge allows to reliably quantify the proportion of four-fold coordinated boron as a function of Li_2O content. The validation of the $^{[4]}B$ quantification by NRIXS is a first step with the objective of applying such methodology in the case of *in situ* experiments or for materials which can be hardly probed by NMR. A spectral feature related to the

presence of NBO(s) on the π^* peak of the B *K*-edge has also been deduced without probing the O *K*-edge. This is particularly relevant in the case of conventional X-ray absorption spectroscopy with which it is less easy than NRIXS, to probe both B and O *K*-edges with the same experimental setup. The spectral feature around 535 eV in the O *K*-edge spectra, ascribed to the presence of NBOs, appears as a key indicator of the polymerization degree of the borate network.

Thanks to the comparative glass/crystal study, we have demonstrated the presence of two sub-domains in LB9 glass relative to a 'Li-rich' domain and a pure B_2O_3 domain containing boroxol rings. Above 20 mol.% Li_2O, the glass structure shows an excess number of NBOs and, above 50 mol.% Li_2O, a deficit of NBOs. This lesser NBO content compared to crystals is mainly related to the presence of a large number of the diborate units in LB glass, whereas a depolymerized network is already seen in its crystalline counterpart, $LiBO_2$. This different behavior is difficult to interpret but a possible answer is in the understanding of the structure of the corresponding liquid and also in the ability of the alkali ions to suit their environment for limiting internal constraints.

Finally, this opens research opportunities for structural characterization of a large variety of boron oxide materials that can be investigated by *in situ* B and O *K*-edges measurements in complex sample environments, such as high-pressure cells or high-temperature furnaces.

5. Acknowledgements

We acknowledge the European Synchrotron Radiation Facility and SOLEIL for provision of synchrotron radiation facilities. (Proposals HD490 and 20130193)

6. References

[1] A. Yamada, N. Iwane, Y. Harada, S. Nishimura, Y. Koyama, I. Tanaka, Adv. Mater. 22 (2010) 3583–3587.
[2] V. Legagneur, Y. An, A. Mosbah, R. Portal, A. Le Gal La Salle, A. Verbaere, D. Guyomard, Y. Piffard, Solid State Ion. 139 (2001) 10.
[3] A.C. Wright, N.M. Vedishcheva, Phys. Chem. Glas. Eur. J. Glass Sci. Technol. B. 57 (2016) 1–14.
[4] A.C. Wright, Int. J. Appl. Glass Sci. 6 (2015) 45–63.
[5] A.C. Wright, Phys. Chem. Glas. Eur. J. Glass Sci. Technol. B. 51 (2010) 233.
[6] A.C. Wright, Phys. Chem. Glas. Eur. J. Glass Sci. Technol. B. 51 (2010) 39.
[7] Borate glasses, crystals & melts: [proceedings of the Second International Conference on Borates Glasses, Crystals and Melt], Society of Glass Technology, Sheffield, 1997.
[8] J. Krogh-Moe, J. Non-Cryst. Solids. 1 (1969) 269–284.
[9] S.A. Feller, W.J. Dell, P.J. Bray, J. Non-Cryst. Solids. 51 (1982) 21–30.
[10] J. Zhong, P.J. Bray, J. Non-Cryst. Solids. 111 (1989) 9.
[11] Y.H. Yun, P.J. Bray, J. Non-Cryst. Solids. 44 (1981) 227–237.
[12] P.J. Bray, J.G. O'Keefe, Phys. Chem. Glas. 4 (1963) 37–46.
[13] E.I. Kamitsos, G.D. Chryssikos, J. Mol. Struct. 247 (1991) 1–16.
[14] E.I. Kamitsos, M.A. Karakassides, G.D. Chryssikos, Phys. Chem. Glas. 28 (1987) 203.

[15] W.L. Konijnendijk, J.M. Stevels, J. Non-Cryst. Solids. 18 (1975) 307–331.
[16] T. Yano, N. Kunimine, S. Shibata, M. Yamane, J. Non-Cryst. Solids. 321 (2003) 137–146.
[17] A.C. Wright, J.L. Shaw, R.N. Sinclair, N.M. Vedishcheva, B.A. Shakhmatkin, C.R. Scales, J. Non-Cryst. Solids. 345–346 (2004) 24–33.
[18] N. Jiang, Solid State Commun. 122 (2002) 4.
[19] N. Jiang, J. Silcox, J. Non-Cryst. Solids. 342 (2004) 12–17.
[20] N. Jiang, J.C.H. Spence, Ultramicroscopy. 106 (2006) 215–219.
[21] J.-P. Rueff, A. Shukla, Rev. Mod. Phys. 82 (2010) 847–896.
[22] C. Sternemann, M. Wilke, High Press. Res. 36 (2016) 275–292.
[23] S.K. Lee, P.J. Eng, H.-K. Mao, Rev. Mineral. Geochem. 78 (2014) 139–174.
[24] G. Lelong, L. Cormier, G. Ferlat, V. Giordano, G.S. Henderson, A. Shukla, G. Calas, Phys. Rev. B. 85 (2012).
[25] C.J. Sahle, C. Sternemann, C. Schmidt, S. Lehtola, S. Jahn, L. Simonelli, S. Huotari, M. Hakala, T. Pylkkanen, A. Nyrow, K. Mende, M. Tolan, K. Hamalainen, M. Wilke, Proc. Natl. Acad. Sci. 110 (2013) 6301–6306.
[26] P. Wernet, D. Nordlund, U. Bergmann, M. Cavalerri, M. Odelius, H. Ogasawara, L.A. Näslund, T.K. Hirsch, L. Ojamäe, P. Glatzel, L.G.M. Pettersson, A. Nilsson, Science. 304 (2004) 5.
[27] G. Lelong, G. Radtke, L. Cormier, H. Bricha, J.-P. Rueff, J.M. Ablett, D. Cabaret, F. Gélébart, A. Shukla, Inorg. Chem. 53(20) (2014) 10903.
[28] G. Rousse, B. Baptiste, G. Lelong, Inorg. Chem. 53 (2014) 6034.
[29] M.D. Mathews, A.K. Tyagi, P.N. Moorthy, Thermochim. Acta. 319 (1998) 9.
[30] A. Kirfel, G. Will, R.F. Stewart, Acta Crystallogr. B39 (1983) 11.
[31] V.F. Stewner, Acta Crystallogr. B27 (1971) 7.
[32] M. He, H. Okudera, A. Simon, J. Köhler, S. Jin, X. Chen, J. Solid State Chem. 197 (2013) 5.
[33] R. Verbeni, T. Pylkkänen, S. Huotari, L. Simonelli, G. Vankó, K. Martel, C. Henriquet, G. Monaco, J. Synchrotron Radiat. 16 (2009) 469–476.
[34] C. Ponchut, J.M. Rigal, J. Clément, E. Papillon, A. Homs, S. Petitdemange, J. Instrum. 6 (2011) C01069–C01069.
[35] J.-P. Rueff, J.M. Ablett, D. Céolin, D. Prieur, T. Moreno, V. Balédent, B. Lassalle-Kaiser, J.E. Rault, M. Simon, A. Shukla, J. Synchrotron Radiat. 22 (2015) 175–179.
[36] S.K. Lee, P.J. Eng, H.-K. Mao, Y. Meng, M. Newville, M.Y. Hu, J. Shu, Nat. Mater. 4 (2005) 4.
[37] M.E. Fleet, S. Muthupari, Am. Mineral. 85 (2000) 12.
[38] G.S. Henderson, F.M.F. de Groot, B.J.A. Moulton, Rev. Mineral. Geochem. 78 (2014) 75–138.
[39] P.J. Bray, J. Non-Cryst. Solids. 95–96 (1987) 15.
[40] S. Kroeker, P.M. Aguiar, Cerquiera, A., Okoro, J., Phys. Chem. Glas. Eur. J. Glass Sci. Technol. B. 47 (2006) 393–396.
[41] P.M. Aguiar, S. Kroeker, J. Non-Cryst. Solids. 353 (2007) 4.
[42] J. Swenson, L. Börjesson, W.S. Howells, Phys. Rev. B. 52 (1995) 9310–9319.
[43] L. Cormier, G. Calas, B. Beuneu, J. Non-Cryst. Solids. 353 (2007) 1779–1784.
[44] E. Ratai, J.C.C. Chan, H. Eckert, Phys. Chem. Chem. Phys. 4 (2002) 3198–3208.
[45] G.E. Jellison, P.J. Bray, J. Non-Cryst. Solids. 29 (1978) 187–206.
[46] M.O.J.Y. Hunault, L. Galoisy, G. Lelong, M. Newville, G. Calas, J. Non-Cryst. Solids. 451 (2016) 101–110.
[47] L. Galoisy, L. Cormier, G. Calas, V. Briois, J. Non-Cryst. Solids. 293–295 (2001) 105–111.
[48] L. Cormier, L. Galoisy, G. Calas, Europhys. Lett. 45 (1999) 572.
[49] E.I. Kamitsos, A.P. Patsis, M.A. Karakassides, G.D. Chryssikos, J. Non-Cryst. Solids. 126 (1990) 52–67.
[50] R.R. Shaw, D.R. Uhlmann, J. Am. Ceram. Soc. 51 (1968) 377–382.
[51] B. Chen, U. Werner-Zwanziger, J.W. Zwanziger, M.L.F. Nascimento, L. Ghussn, E.D. Zanotto, J. Non-Cryst. Solids. 356 (2010) 2641–2644.
[52] G.D. Chryssikos, E.I. Kamitsos, A.P. Patsis, M.S. Bitsis, M.A. Karakassides, J. Non-Cryst. Solids. 126 (1990) 42–51.
[53] G. Ferlat, A.P. Seitsonen, M. Lazzeri, F. Mauri, Nat. Mater. 11 (2012) 925–929.
[54] G. Ferlat, T. Charpentier, A.P. Seitsonen, A. Takada, M. Lazzeri, L. Cormier, G. Calas, F. Mauri, Phys. Rev. Lett. 101 (2008) 4.